LEVEL

AD A074802

NORTHWESTERN UNIVERSITY

DEPARTMENT OF MATERIALS SCIENCE

Technical Report No. 25
September 7, 1979

Office of Naval Research
Contract N00014-75-C-0580
NR 031-733

ANOMALIES IN X-RAY RESIDUAL STRESS MEASUREMENTS IN COLD-ROLLED STEELS

by

H. Dölle and J. B. Cohen

EVANSTON, ILLINOIS

ANOMALIES IN X-RAY RESIDUAL STRESS MEASUREMENTS IN COLD-ROLLED STEELS

by

H. Dölle° and J. B. Cohen*

ABSTRACT

In residual stress measurements with x-rays, the interplanar spacing is assumed to alter monotonically with the tilt (ψ) of the specimen to the x-ray beam; the calculation of the stresses is based on this assumption when either the well-known two-tilt or $\sin^2\psi$ methods are employed. But in materials with strong texture, large oscillations have sometimes been reported. A method proposed in the literature for evaluating stresses in such a situation as resulting from anisotropy has been tested and shown to provide a reasonable stress system; the texture must be known in detail. so as to calculate the effective elastic constants. More importantly, the theory predicts that the simpler methods and measured x-ray elastic constants <u>can</u> be used, and without knowledge of the texture, <u>if</u> hoo and hhh reflections are employed; this has been verified experimentally in this study. It is recommended that such reflections be employed in the future, rather than the common ones now utilized.

°H. Dölle, formerly Post-doctoral Visiting Scholar, Northwestern University, is now with Brown, Boveri and Cie, Baden, Switzerland and *J. B. Cohen is Frank C. Engelhart Professor of Materials Science and Engineering, Technological Institute, Northwestern University, Evanston, Illinois 60201.

INTRODUCTION

The calculation of stresses from strains observed in polycrystalline materials by X-ray diffraction is a well-established procedure.[1, 2] When a polycrystalline specimen is subjected to stresses the average interplanar spacing ("d") in each crystallite in the aggregate changes. However, because of the elastic anisotropy of the crystallites and their mutual coupling, deviations from the average may occur. Furthermore, the measurement is selective in the sense that only those grains or subgrains properly oriented to diffract contribute to the diffraction profile. Both of these factors imply that the X-ray elastic constants (which link the measured strains to the stresses) depend on the particular $hk\ell$ reflection chosen for the measurement of the "d" spacing.[3, 4] Even when the material has no texture, a dependence on $hk\ell$ can exist[4], and this is one reason why in practice the constants are often measured for a specific material rather than calculating them. Theory[1, 2, 4] predicts that "d" vs $\sin^2\psi$ should vary linearly with a slope that depends on the stress system; here ψ is the angle between the normal (L_3) to the diffracting planes and the normal to the specimen's surface ($\underline{P}_3$) as shown in Fig. 1. Curvature can occur in such plots if there are strong stress gradients, but these are not the subject of this paper. (A review of such phenomena can be found in refs. 4, 5.) Here we wish to consider the large <u>oscillations</u> in "d" vs. $\sin^2\psi$ which have been reported in textured materials by many investigators.[6-11] (An example will be seen in subsequent figures, such as Fig. 6.) It is important to understand these oscillations so as to be able to perform stress measurements with confidence in such materials.

The possibility of oscillations in d vs. $\sin^2\psi$ in <u>randomly</u> oriented polycrystals was first discussed by Greenough.[12] He based his approach on the fact that during deformation different amounts of yielding occur due to

differences in the orientations of the grains. When the load is removed each grain contracts elastically and intergranular microscopic strains develop. These strains are superimposed on those due to macrostresses which he considered to produce a linear d vs. $\sin^2\psi$ relationship.

The first interpretation of nonlinearities in <u>textured</u> materials was given by Bollenrath, Hauk and Weidemann[6] and subsequently extended by Marion and Cohen.[9] These authors considered the cause of the oscillations to be a change in strains with ψ tilt, because grains in certain orientations are able to yield to relieve the applied stresses, or to rotate to do so. This selective (dynamic) recovery of local strains leads to oscillations in "d" spacing superimposed on an average value caused by the macrostress system.

There is one experimental result[10] which is in conflict with this interpretation: When an annealed specimen, with strong texture, is deformed by small elastic tensile loads, oscillations occur, and these vanish when the load is removed. This result does however support the proposals, by Shiraiwa and Sakamoto[8] and Dölle and Hauk[13], that these oscillations in d vs. $\sin^2\psi$ are due to elastic anisotropy. That is, these authors propose that the X-ray elastic constants vary with Φ and ψ tilt in a material with a strong texture, because grains with different orientations are sampled at each such tilt. Such oscillations occur with Al[10] which has half the anisotropy of iron, and indeed these oscillations are a half or less than those observed with steels. Of course, oscillations due to local stress relief can also superimpose on the oscillations due to anisotropy.

Unfortunately, with the approach due to anisotropy it is necessary to calculate the six anisotropic elastic constants; quite difficult and lengthy experiments would be required to measure them in practice. Furthermore, calculations can be readily carried out only by interpreting the actual texture in terms

of ideal components.[4, 13] Nonetheless, such calculations have been shown to be in qualitative agreement with the observed oscillations, for example, for steel, the 211 reflection and CrK_α radiation.[8-11]

One result of the calculations[4, 13] is that the X-ray elastic constants for hoo and hhh reflections are independent of Φ and ψ. The "d" spacing should again be linear vs $\sin^2\psi$, as for quasi-isotropic materials. Thus if practice with steel was changed to employ, say, the 222 reflection with CuK_α (near $140^\circ 2\theta$) and a solid state detector or diffracted beam-monochromator to eliminate fluorescence, the standard two-exposure method or the slope of "d" vs $\sin^2\psi$ could be employed to obtain the stresses, and the effective elastic constants could again be readily measured.

It is the purpose of this paper to test this proposal. In addition, the method of calculating the elastic constants vs Φ, ψ and obtaining the stresses will be given, in case it is necessary to examine reflections that show such oscillations. This theory is shown here for the first time to agree quantitatively with the measurements.

THEORY

It will be assumed that the material is cubic. Various orthonormal co-ordinate systems will be employed and these are illustrated in Fig. 2. For example, the matrix ω between P_i and L_i in Fig. 1 can be written as:

$$\underline{\omega} = \begin{pmatrix} \cos\Phi\cos\psi & \sin\Phi\cos\psi & -\sin\psi \\ -\sin\Phi & \cos\Phi & 0 \\ \cos\Phi\sin\psi & \sin\Phi\sin\psi & \cos\psi \end{pmatrix}. \qquad [1]$$

The rows of the matrix are the components of the vectors of the laboratory system $\underline{L}_i$ in terms of the specimen's sytem $\underline{P}_i$. This is ndicated by the arrows in Fig. 2. (That is, the first row is L_1 in terms of P_1, P_2, P_3.)

Primed stress and strain components will refer to measurements in the Laboratory system $\underline{L}_i$ unprimed in the specimen system. Thus the stress in direction $\underline{L}_i$ can be written in terms of these in $\underline{P}_i$ as:

$$\sigma'_{ij} = \omega_{ik}\omega_{j\ell}\sigma_{k\ell}$$

A general three dimensional stress tensor will be considered:

$$\underline{\sigma} = \begin{pmatrix} \sigma_{11} & \sigma_{12} & \sigma_{13} \\ \sigma_{12} & \sigma_{22} & \sigma_{23} \\ \sigma_{13} & \sigma_{23} & \sigma_{33} \end{pmatrix} \quad . \qquad [2]$$

Note that σ_{33}, σ_{23}, and σ_{13} are components normal to the surface of the specimen; these are often assumed to be zero in stress measurements with x-rays, but over the depth of penetration of the beam, if there are large gradients, these terms can be detected.(4, 14, 15) A particular ideal preferred orientation of a texture will be written as $(n_1n_2n_3)[w_1w_2w_3]$, implying that n_i is the crystal plane parallel to the rolled surface and w_i is the rolling direction.

The strain $\langle\epsilon'_{33}\rangle$, with carats indicating averaging over the crystallites reflecting in the direction Φ, ψ or L_3 in Fig. 1, can be written as:

$$\langle\epsilon'_{33}\rangle \equiv \langle\frac{d_{\Phi\psi} - d_o}{d_o}\rangle = \langle(s'_{33ij} + t'_{33ij}) \cdot \sigma'_{ij}\rangle, \qquad [3]$$

where:

$d_{\Phi\psi}$ = interplanar spacing for the direction $\underline{L}_3$,

d_o = interplanar spacing of a stress-free specimen,

ϵ'_{33} = strain normal to the planes $\{hk\ell\}$,

s'_{33ij} = single crystal compliances in the system $\underline{L}_i$,

t'_{33ij} = elastic interaction of a grain and its surrounding matrix(16-18, 19)

σ'_{ij} = stress components in system $\underline{L}_i$.

(Repeated subscripts imply summation.)

If the number of crystallites reflecting is large:

$$\langle \epsilon'_{33}\rangle = \langle (s'_{33ij} + t'_{33ij})\cdot\sigma'_{ij}\rangle = \langle (s'_{33ij} + t'_{33ij})\rangle\cdot\langle\sigma'_{ij}\rangle =$$

$$(\langle s'_{33ij}\rangle + \langle t'_{33ij}\rangle)\cdot\langle\sigma'_{ij}\rangle \quad . \qquad [4]$$

$$= R'_{ij}\ \langle\sigma'_{ij}\rangle . \qquad [5]$$

The calculations of the anisotropic x-ray elastic constants will be done in the Reuss limit,[20] in which the interaction term t'_{33ij} is neglected so that the same (uniform) stresses, σ_{ij}, are assumed to act on all the crystallites. Let λ^i be the volume fraction of unoriented crystallites and λ^a the volume fraction of a particular ideal component of the texture. In practice, these fractions are obtained from the variation with ψ and Φ of the intensity of the hkℓ peak being measured, as illustrated in Fig. 3. With this information it will be assumed that:

$$R'_{ij}(hk\ell,\Phi,\psi) = \frac{\lambda^i r_{ij}(hk\ell) + \Sigma\lambda^a\langle s'_{33ij}\rangle^a}{\lambda^i + \Sigma\lambda^a} \quad . \qquad [6]$$

Here, the isotropic terms r_{ij} depend on the x-ray elastic constants $s_1(hk\ell)$ and $\frac{1}{2}\, s_2(hk\ell)$ as follows:[21]

$$r_{11}(hk\ell) = r_{22}(hk\ell) = s_1(hk\ell) \qquad [7a]$$

$$r_{33}(hk\ell) = s_1(hk\ell) + \tfrac{1}{2}\, s_2(hk\ell) \qquad [7b]$$

$$r_{12}(hk\ell) = r_{13}(hk\ell) = r_{23}(hk\ell) = 0 \qquad [7c]$$

In this study, the x-ray elastic constants s_i were calculated in Kroner's approximation[18] (see also ref. 4). The single crystal compliances (of Fe) were taken from ref. 22.

The calculation of R_{ij} vs Φ, ψ, proceeds as follows, referring to Fig. 2 (see the appendix for details):

1. The orientation of the cut of the specimen relative to the rolling system is noted. This defines the matrix elements η_{ij}, which are the direction

cosines between the axes of the specimen, $\underline{P}_i$, and the natural axes of the texture $\underline{B}_j$.

2. An $hk\ell$ reflection is chosen to be measured.

3. All planes in its form and the unit vector $\underline{L}_3$ normal to these planes are listed.

4. For one ideal component of the texture, the matrix elements β_{ij}, which describe the crystal orientation with respect to the co-ordinate system of the rolling process, $\underline{B}_i$, are calculated.

5. The components π_{ij} of the specimen's axes in terms of crystal co-ordinates are $\eta_{ik}\cdot\beta_{kj}$.

6. The values of Φ,ψ are calculated for every $hk\ell$ in the form, for this ideal component of the texture.

7. For each reflection the matrix γ is obtained.

8. With the matrix elements γ_{ij} the transformed single crystal compliances s'_{33ij} are calculated:

$$s'_{33ij} = \gamma_{3m}\cdot\gamma_{3n}\gamma_{io}\gamma_{jp}\cdot s_{mnop}. \qquad [8]$$

9. After all the ideal components of the texture are considered as in 4-8, s'_{33ij} is summed at each Φ,ψ, and R'_{ij} is calculated, following Eq. 6.

In the Appendix, it is also shown that the x-ray elastic constants will be independent of Φ and ψ for hoo and hhh-type reflections.

From Eqs. 1, 5, 6 and 8, the variation in strains due to elastic anisotropy can be calculated. Consider a (211) plane reflecting; $\underline{L}_3 = \frac{1}{\sqrt{6}}\begin{pmatrix}2\\1\\1\end{pmatrix}$. The compliances s'_{33ij} depend on which crystallographic direction is parallel to $\underline{L}_2$. Four orientations will be assumed here, $\pm\frac{1}{\sqrt{2}}[0\bar{1}1]$ and $\pm\frac{1}{\sqrt{3}}[\bar{1}11]$, see Fig. 4. (The unit vector $\underline{L}_1$ can be obtained from $\underline{L}_1 = \underline{L}_2 \times \underline{L}_3$.) With $\lambda^i = 0$ and the elastic compliances for Fe, the results listed in Table I were obtained. The variations of R and ε' with ψ tilt are of the same magnitude as the experimental

data for iron and steel[3, 6-11] and are three times larger than the values calculated in previous approaches which assumed no texture.[12] It is clear that this approach can be applied quantitatively, and this is done in what follows.

EXPERIMENTAL PROCEDURES

From hot-rolled plates of a plain low-carbon steel (annealed for 12 h at 1300^{o} in air and furnace cooled), sheets 250 x 100 x 8 mm were taken and reduced by cold rolling to a final thickness of 2 mm in 40 passes, reversing the sheets end for end after each pass.

The chemical analysis of the steel gave the following composition (in wt pct.): C: 0.10; Si: 0.34; Mn: 1.34; S: 0.025; Cr: 0.04; Ni: 0.06; Cu: 0.16; Mo: 0.01. (The microstructure and the texture can be found in ref. 11). In the rolling direction the yield strength is 758 MPa, and the tensile strength is 849 MPa, with an elongation of 6 pct. Specimens cut at 45^{o} to the rolling direction exhibited stress values $\approx$ 10 pct. lower.

Two strips were examined in this study, one cut from a sheet with its longitudinal direction P_1 parallel to the rolling direction $\underline{B}_1$, and another at -45^{o} to this direction.

For the x-ray measurements, a G.E. XRD-5 diffractometer was employed, equipped with a quarter circle goniometer, a pulse height analyzer and a scintillation detector. The ψ-tilt and the 2θ-rotation were controlled by a minicomputer, in a step-scan mode.[23] Intensities were corrected for the Lorentz-polarization factor, after which the peak position (and hence the "d" spacing) was obtained with a five-point parabolic fit to the highest 15 pct. of the peak. The positions were corrected for variations in peak shape with ψ.[5] An annealed Cr powder dusted on a specimen was employed to align the specimen by adjusting its position until 2θ at the peak was independent of ψ. Also corrections from the actual 2θ to the true 2θ were obtained from this powder. Because interplanar spacings were measured at both high and

intermediate 2θ values, large ψ tilts could not be carried out around the θ axis. Instead of this, the tilt was about an axis parallel to the plane of diffraction.[24] (This experimental arrangement is referred to as a "ψ goniometer" in Europe). For this tilt, no absorption correction is required. Circular collimators, 95 mm long with 2.2 mm diameter openings were used for the incident and diffracted beams. Attempts to use openings of 1 mm in size indicated that there was too much scatter due to the elongated grains. Vanadium filtered CrK_α (50 kv, 16 ma) was employed and the 200 and 211 reflections were examined. Twenty-one ψ tilts (0, $\pm$ 13°, $\pm$ 19.5, $\pm$ 22.8, $\pm$ 26.6, $\pm$ 30, $\pm$ 33.6, $\pm$ 35.6, $\pm$ 38.5, $\pm$ 42, $\pm$ 45), were employed, each at four angles from the rolling direction, 0°, 60°, 90°, 120°. Each measurement was repeated four times and averaged. The range of values will be indicated with the results.

RESULTS AND DISCUSSION

The variation of intensities and lattice strains with $\sin^2\psi$, in different directions relative to the rolling direction, is shown in Fig. 5 for the 200 reflection, and in Fig. 6 for the 211 reflection. The values shown are averages for $\pm\psi$. Differences in strains for $+\psi$ and $-\psi$ are caused by shear stresses σ_{13} and σ_{23} and for isotropic materials there is a linear dependence of the difference on $\sin|2\psi|$.[4, 5, 15] Such shear residual stresses are zero at the surface, but they can contribute if there are strong gradients over the depth of penetration of the x-ray beam. An examination of the data at $\pm\psi$ for the 200 reflection revealed that there was no $\sin|2\psi|$ dependency.

Note particularly that significant oscillations occur only for the rolling direction and the 211 reflection (Fig. 6), despite the fact that there is considerable texture as indicated by the variations in intensities in both Figs. 5 and 6. It is quite clear that the predictions of the theory discussed in this

paper (that attributes these oscillations to elastic anisotropy) seems to be correct, because the 200 reflection shows no such effects.

The strains were calculated by assuming a lattice parameter $a_o = .28665$ nm for stress-free iron. (This is the value that has been found to be suitable in many studies.[25]) For a first evaluation of the stresses only the terms σ_{11}, σ_{12}, σ_{22} were considered. That is, a surface stress state was assumed. The stress system was evaluated from both reflections. First, for the 211 reflection, the volume fractions λ^i and λ^a were obtained from Fig. 6, as indicated in Fig. 2. Five ideal components were assumed to be adequate to describe the texture:[17] (211)[01$\bar{1}$]; (211)[0$\bar{1}$1]; (111)[$\bar{2}$11]; (111)[2$\bar{1}\bar{1}$]; (100)[011]. The anisotropic elastic constants R'_i, were then calculated at all the Φ, ψ used in the measurements. The stresses in the sample co-ordinates P_i were then evaluated from:

$$\begin{aligned}\langle\epsilon'_{33}\rangle = {} & [R'_{11}\cos^2\Phi\cos^2\psi + R'_{22}\sin^2\Phi + R'_{33}\cos^2\Phi\sin^2\psi - R'_{12}\sin2\Phi\cos\psi + R'_{13}\cos^2\Phi\sin2\psi \\ & - R'_{23}\sin2\Phi\sin\psi]\langle\sigma_{11}\rangle + [R'_{11}\sin^2\Phi\cos^2\psi + R'_{22}\cos^2\Phi + R'_{33}\sin^2\Phi\sin^2\psi + \\ & R'_{12}\sin2\Phi\cos\psi + R'_{13}\sin^2\Phi\sin2\psi + R'_{23}\sin2\Phi\sin\psi]\langle\sigma_{22}\rangle + [R'_{11}\sin2\Phi\cos^2\psi - \\ & R'_{22}\sin2\Phi + R'_{33}\sin2\Phi\sin^2\psi + 2R'_{12}\cos2\Phi\cos\psi + R'_{13}\sin2\Phi\sin2\psi + \\ & 2R'_{23}\cos2\Phi\sin\psi]\langle\sigma_{12}\rangle . \end{aligned} \qquad [9]$$

For the 211-reflection a least-squares fit to the measured strains was made to those 18 points listed in Table II where anisotropic x-ray elastic constants could be calculated from the intensities vs Φ, ψ (because these components yield 211 poles at these angles). The resulting stress tensor (in MPa) is:

$$\begin{pmatrix} -360 & -67 & 0 \\ -67 & -405 & 0 \\ 0 & 0 & 0 \end{pmatrix} . \qquad [10]$$

The open circles in Fig. 6 are values back-calculated from this tensor. For the 200 reflection it has been shown that there are no oscillations, and

therefore isotropic theory was employed to evaluate stresses. For hoo and hhh-type reflections the x-ray elastic constants R'_{12} R'_{13} and R'_{23} are zero, and using Eq. 7 the stress-strain relationship for these reflections is (for a surface stress state):

$$\langle \varepsilon'_{33} \rangle = \tfrac{1}{2}\, s_2(hk\ell)[\langle\sigma_{11}\rangle \cos^2\phi + \langle\sigma_{12}\rangle \sin 2\phi + \langle\sigma_{22}\rangle \sin^2\phi]\sin^2\psi$$
$$+ s_1(hk\ell)[\langle\sigma_{11}\rangle + \langle\sigma_{22}\rangle]. \qquad [11]$$

The stress tensor (in MPa) resulting from a least-squares solution of the 63 entries in Table II (for the data at $\phi = 0^o$, 60^o, 90^o) is:

$$\begin{pmatrix} -526 & -72 & 0 \\ -72 & -542 & 0 \\ 0 & 0 & 0 \end{pmatrix} . \qquad [12]$$

For comparison, the more traditional method(1, 2) of obtaining the stress from $\frac{\partial\langle \varepsilon'_{33}\rangle}{\partial \sin^2\psi}$ was examined. For the 200 reflection at $\phi = 0^o$, $\sigma_{11} = -531$ MPa, at $\phi = 90^o$, $\sigma_{22} = -544$ MPa. For the 211 reflection, $\phi = 90^o$, $\sigma_{22} = -292$ MPa. (At $\phi = 0^o$ for this reflection there are strong oscillations and this evaluation was not possible.) The errors were estimated to be less than $\pm$ 10 pct. from solutions with the data on the annealed Cr powder. Except for the last value there is good agreement between all the methods.

CONCLUSIONS

So far it has been assumed that a surface stress state existed in the specimen. When a three-dimensional stress state was employed for the calculations, the shear stresses σ_{13}, σ_{23} were within the error estimate, the normal stress σ_{33} was tensile ($\approx$ 100 - 200 MPa) and σ_{11}, σ_{22} were less compressive by about the same amount. However, the agreement between the two reflections was poor.

It should be emphasized that oscillations can occur if the grain size is too coarse. This can sometimes be distinguished from the true anomalies, by

removing the specimen and remeasuring after replacing it. If the effect is due to grain size the location of the oscillations in d vs $\sin^2$ can change considerably, but the intensity will certainly vary.

The results reported here support the interpretation that oscillations in lattice strain vs $\sin^2\psi$ in textured materials are mainly due to the combined effects of texture and elastic anisotropy. Furthermore, these effects can be minimized by choosing an hoo or hhh reflection. While it has been demonstrated here that stresses can be obtained even when oscillations are present, the measurements and analysis are much simpler and more rapid when $\langle\epsilon'_{33}\rangle$ vs $\sin^2\psi$ is linear. Therefore consideration should be given to changing current practice for stress measurements from the usual peaks to hoo or hhh types. Also, the method described in this paper that takes into account texture and anisotropy involves calculating elastic constants. But it is well known[(3)] that these constants can vary appreciably with the amount of plastic deformation. Change of as much as 20-40 pct. has been reported. Until this problem is understood it is better to employ methods that can utilize measured values of the elastic constants $s_1(hk\ell)$ and $\frac{1}{2}\,s_2(hk\ell)$. From Eq. 11 it is clear that these values can be obtained by elastically loading to known stresses and measuring $\langle\epsilon'_{33}\rangle$. This practice has in fact often been followed with the more traditional reflections and should cause no problems with the new reflections suggested by this study.

ACKNOWLEDGEMENTS

This work was supported by ONR under grant no. 00014-75-C-0580. The measurements were carried out in the Long Term X-ray Facility of Northwestern University's Materials Research Center, supported in part by NSF grant no. DMR 76-80847. The specimens were prepared at the "Institut für Bildsame Formgebung" and the "Institut für Werkstoffkunde" of TH. Aachen, Germany. One of us (H.D.) would like to thank the Council of International Exchange of Scholars (Fulbright-Hays program) for a travel grant.

APPENDIX

We follow the nine steps listed in the manuscript to calculate R'_{ij}, eqn. 6.

1. Calculate matrix elements η_{ij} linking the directions the sample is cut with respect to the rolling co-ordinates.

2. Consider a 211 reflection.

3. One component of the form of the reflecting planes, e.g. $(1\bar{2}1)$ is taken; for this plane, $\underline{L}_3 = \frac{1}{\sqrt{6}}[1\bar{2}1]$.

4. For the component of the preferred orientation $(n_1n_2n_3)[w_1w_2w_3]$, the matrix elements of $\underline{\beta}$ in Fig. 2 are formed.

$$B_{11} = \frac{w_1}{(w_1^2 + w_2^2 + w_3^2)^{\frac{1}{2}}};\ B_{12} = \frac{w_2}{(w_1^2 + w_2^2 + w_3^2)^{\frac{1}{2}}};\ B_{13} = \frac{w_3}{(w_1^2 + w_2^2 + w_3^2)^{\frac{1}{2}}} \quad \text{(A-1a)}$$

$$B_{31} = \frac{n_1}{(n_1^2 + n_2^2 + n_3^2)^{\frac{1}{2}}};\ B_{32} = \frac{n_2}{(n_1^2 + n_2^2 + n_3^2)^{\frac{1}{2}}};\ B_{33} = \frac{n_3}{(n_1^2 + n_2^2 + n_3^2)^{\frac{1}{2}}}, \quad \text{(A-1b)}$$

$$B_{21} = B_{13}B_{32} - B_{12}B_{33}\ ;\ B_{22} = B_{11}B_{33} - B_{13}B_{31}\ ;\ B_{23} = B_{12}B_{31} - B_{11}B_{22}. \quad \text{(A-1c)}$$

The B_{ij} are the projections of the $\underline{B}_i$ axes onto the $\underline{A}_i$ crystal axes. The axis $\underline{B}_1$ has the indices of the rolling direction, $\underline{B}_3$ the indices of the normal to the rolling plane.

5. The matrix elements $\pi_{ij} = \eta_{ik}\beta_{kj}$ are the components of the specimens axes, $\underline{P}_i$, in terms of the crystal ordinates, A_i.

6. For each $(hk\ell)$ in the form $\{hk\ell\}$,

$$\tan\Phi = \frac{q_2}{q_1}, \quad \text{(A-2a)}$$

$$\sin^2\psi = q_1^2 + q_2^2, \quad \text{(A-2b)}$$

where:

$$q_1 = \underline{P}_1 \cdot \underline{L}_3, \quad \text{(A-3a)}$$

$$q_2 = \underline{P}_2 \cdot \underline{L}_3 . \quad \text{(A-3b)}$$

Here, $\underline{P}_1$ is the first row of the matrix π, $\underline{P}_2$, the second row.

7. The direction $\underline{L}_2$ in Fig. 1 can then be obtained from:

$$\underline{L}_2 = \begin{pmatrix} \gamma_{21} \\ \gamma_{22} \\ \gamma_{23} \end{pmatrix} = \begin{pmatrix} \cos\Phi & \sin\Phi & 0 \\ -\sin\Phi & \cos\Phi & 0 \\ 0 & 0 & 1 \end{pmatrix} \begin{pmatrix} \pi_{21} \\ \pi_{22} \\ \pi_{23} \end{pmatrix} \tag{A-4}$$

The last (column) matrix is $\underline{P}_2$ in terms of the crystal axes, $\underline{A}_i$;hence $\underline{L}_2$ is simply $\underline{P}_2$ rotated Φ around $\underline{P}_3$, as can be seen in Fig. 1. The vector $\underline{L}_1$ is then obtained from the cross product:

$$\underline{L}_1 = \underline{L}_2 \times \underline{L}_3 = \begin{pmatrix} \gamma_{11} \\ \gamma_{12} \\ \gamma_{13} \end{pmatrix} \tag{A-5}$$

The elements of γ_{31}, γ_{32}, γ_{33} are $\frac{1}{6}\,[1\bar{2}1]$, i.e. the direction L_3 in terms of the crystal axes, A_3.

8. Having thus obtained all the elements of the matrix γ (see Fig. 2), for a given component of the texture and a given $hk\ell$ in the form $\{hk\ell\}$, the s'_{33ij} can be calculated for this Φ,ψ with Eqn. 8. This equation can be simplified to the form:

$$s'_{33ij} = s_{1122}\delta_{ij} + 2s_{1212}\delta_{3i}\delta_{3j} + s_o\gamma^2_{3k}\,\gamma_{ik}\gamma_{jk} \tag{A-6a}$$

Where δ_{ij} is the Kronecker delta function. ($\delta_{ij} = 0,\ i \neq j,\ \delta_{ij} = 1,\ i = j$)

Also: $s_o \equiv s_{1111} - s_{1122} - 2s_{1212}$. (A-6b)

9. The steps 3 through 7 are repeated for the next ideal component of the preferred orientation and then at each Φ, ψ, $\langle s'_{33ij}\rangle$ is obtained.

From Eqn. A-6a it can be shown that for hoo and hhh reflections, $\langle s'_{33ij}\rangle^a$ reduces to the quasi-isotropic term $r'_{ij}(hk\ell)$ in Eqn. 6. For hoo reflections, the vectors $\underline{L}_i$ are $\underline{L}_1 = [100]$, $\underline{L}_2 = [010]$, and $\underline{L}_3 = [001]$. The last term in Eqn. A-6a therefore vanishes, except for $i = j = 3$. For hhh reflections, all components of $\underline{L}_3$ are $\frac{1}{3}\sqrt{3}$ and, since $\underline{L}_1$ and $\underline{L}_2$ are orthogonal, the last term in Eqn. A-6 is zero unless $i = j$.

REFERENCES

1. B. D. Cullity: Elements of X-ray Diffraction, Addison-Wesley, Reading, Mass., 1956.

2. C. S. Barrett and T. B. Massalski: Structure of Metals, 3rd ed., McGraw-Hill, New York, 1966.

3. R. H. Marion and J. B. Cohen: Adv. in X-ray Anal., 1977, vol.20, pp. 335-367.

4. H. Dölle: J. Appl. Cryst.,in print.

5. M. R. James and J. B. Cohen: "The Measurement of Residual Stress by X-ray Diffraction Techniques;" in <u>Advances in Materials Research</u>, (H. Herman ed.), Academic Press, New York; in press.

6. F. Bollenrath, V. Hauk and W. Weidemann: Arch. Eisenhuttenwes., 1967, vol. 38, pp. 793-800.

7. F. Bollenrath, V. Hauk and W. Ohly: Härterei Techn. Mitt., 1968, vol. 23, pp.311-313.

8. T. Shiraiwa and Y. Sakamoto: Proc. 13th Jap. Congr. on Mater. Res. Metal Mater., Kyoto, 1970, pp. 25-32.

9. R. H. Marion and J. B. Cohen: Adv. in X-ray Anal., 1975, vol. 18, pp. 466-501.

10. V. Hauk. D. Herlach and H. Sesemann: Z. Metallkde. 1975, vol. 66, pp. 734-737.

11. H. Dölle, V. Hauk and H. Zegers: Z. Metallkde., 1978, vol. 69, pp. 766-772.

12. G. B. Greenough: Proc. Royal Soc., 1949, vol. 197A, pp. 556-567.

13. H. Dölle and V. Hauk: Z. Metallkde., 1978, vol. 69, pp. 410-417.

14. H. Dölle and V. Hauk: Härterei Techn. Mitt., 1976 vol.31 pp. 165-168.

15. H. Dölle and J. B. Cohen: Met. Trans., in press.

16. S. M. Wecker and P. R. Morris: J. Appl. Cryst.,1978, vol. 11, 211-220.

17. G. Wassermann and J. Greven: Texturen metallischer Werkstoffe, 2nd ed., Springer, Berlin, 1962.

18. E. Kröner: Z. Physik, 1958, vol. 151, pp. 504-518.

19. P. R. Morris: Int. J. Engng. Sci., 1970, vol. 8 pp. 49-61.

20. A. Reuss: Z. Angew. Math. in Mech., 1929, vol. 9, pp.49-58.

21. H. Möller and G. Martin: Mitt. V. W. I. Eisenforschg. Düsseldorf, 1939, vol. 21, pp 261-269.

22. Landolt-Börnstein, Group III, vol.2: Crystal and Solid State Physics, ed. K. - H. Hellwege, Springer, Berlin-Hiedelberg-New York, 1969.

23. M. R. James and J. B. Cohen: Adv. in X-ray Anal., 1977, vol. 20, pp. 291-309.

24. E. Macherauch and U. Wolfstieg: Adv. in X-ray Anal., 1977, vol. 20 pp. 369-378.

25. G. Faninger, V. Hauk, E. Macherauch and U. Wolfstieg: Härterei-Techn. Mitt., vol. 31, 1976, 109-111.

26. H. Dölle and V. Hauk: submitted for publication to Z. Metallkde.

TABLE I

X-ray elastic constants R'_{ij} and lattice strains ϵ'_{33} for crystallites with different orientations. R'_{ij} has been calculated with $\lambda^i = 0$ and σ'_{ij} can be calculated from equations 5,6, and 8; $\Phi = 0$, Reuss-limit.

Orientation $\underline{L}_2$	$\frac{1}{3}[1\bar{1}\bar{1}]$	$\frac{1}{3}[\bar{1}11]$	$\frac{1}{2}[0\bar{1}1]$	$\frac{1}{2}[01\bar{1}]$	isotropic * polycrystal calculated following ref. 21
R'_{11}	-1.80	-1.80	- .78	- .78	
R'_{22}	- .78	- .78	-1.80	-1.80	-1.29
R'_{33} (in $10^{-6}MPa^{-1}$)	4.59	4.59	4.59	4.59	4.59
R'_{12}	0	0	0	0	0
R'_{13}	0	0	1.44	-1.44	0
R'_{23}	1.44	-1.44	0	0	0
$\epsilon'_{33}(\psi = 0)$ in 10^{-4} for $\sigma_{11} = -100$ MPa	1.80	1.80	.78	.78	1.29
$\epsilon'_{33}(\psi = 0)$ in 10^{-4} for $\sigma_{11} = \sigma_{22} = -100$ MPa	2.58	2.58	2.58	2.58	2.58
$\epsilon'_{33}(\psi = 15^{o})$ in 10^{-4} for $\sigma_{11} = -100$ MPa	1.35	1.35	- .31	1.13	.88
$\epsilon'_{33}(\psi = 15^{o})$ in 10^{-4} for $\sigma_{11} = -100$ MPa	1.35	1.35	1.13	.31	.88
$\epsilon'_{33}(\psi = 15^{o})$ in 10^{-4} for $\sigma_{11} = \sigma_{22} = -100$ MPa	2.13	2.13	2.93	1.49	2.17

*This column is also the average of columns 2-5, but only because of the special orientations assumed for the calculations.

TABLE II

Angles of measurement and contributing preferred orientations.

a: $(211)[01\bar{1}]$ or $(211)[0\bar{1}1]$

b: $(111)[\bar{2}11]$ or $(111)[2\bar{1}\bar{1}]$

c: $(100)[011]$

ψ \ * Φ'	0^o	60^o	90^o	120^o
0	a	a	a	a
±13				
±19.5	b	b		b
±22.8				
±26.6				
±30				
±33.6		a		a
±35.3	c		c	
±38.5				
±42				
±45				

* Φ' is the azimuth angle with respect to the rolling direction. For $\psi = 0$ there is a coincidence of both "a" preferred orientations; for the other directions only one of the preferred orientations results in a reflection.

FIGURE CAPTIONS

Fig. 1 Definition of positive Φ and ψ tilt, orientation of the X-ray beam and the laboratory axial system $\underline{L}_i$ with respect to the specimen's system $\underline{P}_i$.

Fig. 2 The various co-ordinate systems and their orientation matrices employed in the text. The arrows indicate the direction that these matrices transform the tensor components.

Fig. 3 Schematic representation of the method used for the evaluation of the isotropic (λ^i) and the different anisotropic (λ^a) volume fraction of the crystallites reflecting. The reflection 211 is considered and the intensity is measured with the rolling direction (RD) normal to the goniometer. The ψ tilt is around the transverse direction. The peaks in intensity are shown due to various components of the texture. The minimum intensity is taken as that due to randomly distributed crystallites.

Fig. 4 Possible orientations of crystallites contributing to the 211-reflection at the direction Φ,ψ. The components of $\underline{L}_1$ and $\underline{L}_2$ are in terms of the crystal co-ordinates ($\underline{A}_i$).

Fig. 5 Relative intensities and lattice strains vs. $\sin^2\psi$, measured for different directions with the 200 reflection. The small bar beneath the point indicates the standard deviation in 4 measurements. The large bar is given to illustrate the error due to a 0.05° uncertainty in 2θ. RD-rolling direction, TD-transverse direction.

Fig. 6 Relative intensities and lattice strains vs. $\sin^2\psi$, measured for different directions with the 211 reflection. The small bar beneath the point indicates the standard deviation in 4 measurements. The large bar is given to illustrate the error due to a 0.05° uncertainty in 2θ. RD-rolling direction, TD-transverse direction.

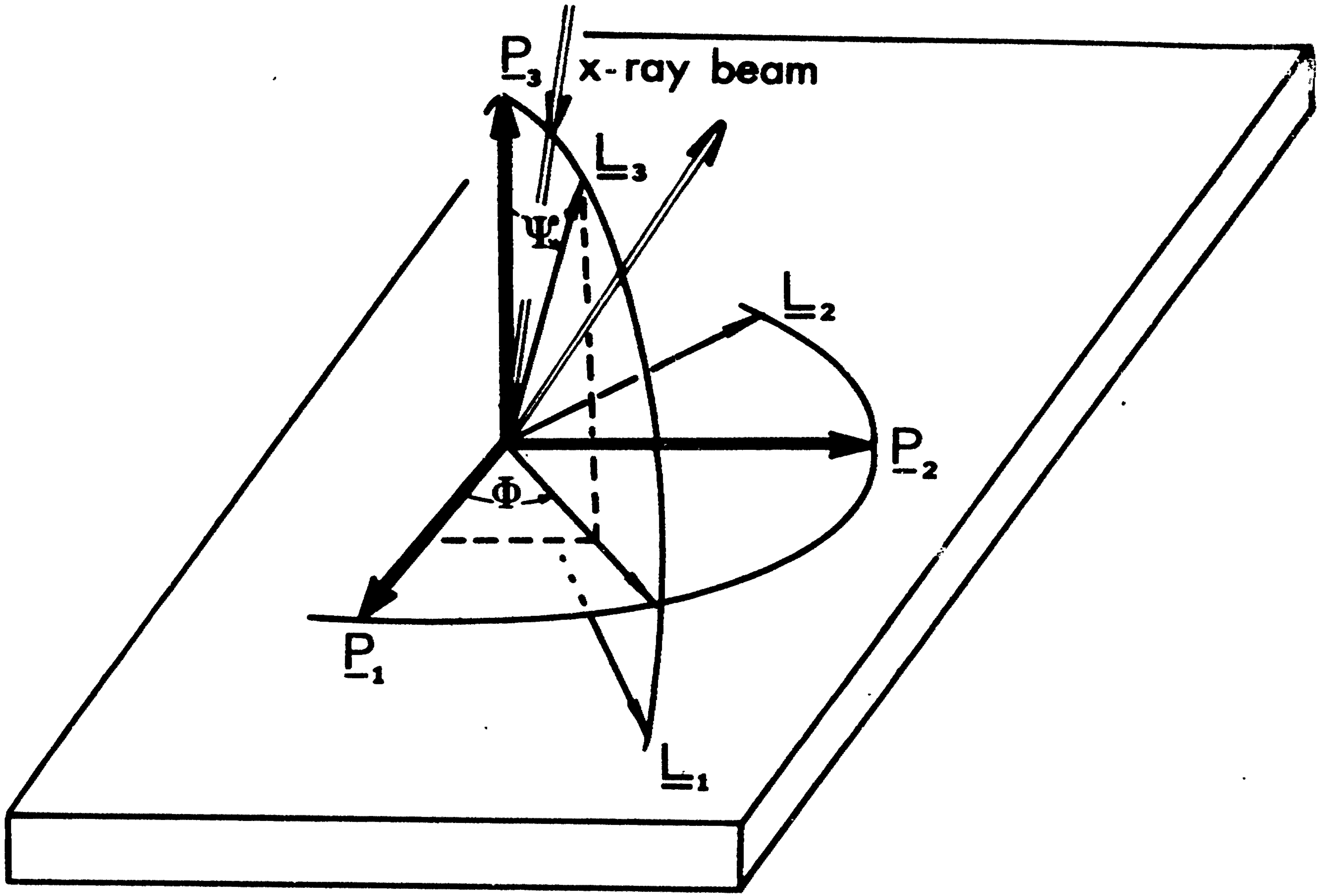

Fig. 1 H. Dölle and J. B. Cohen

fig

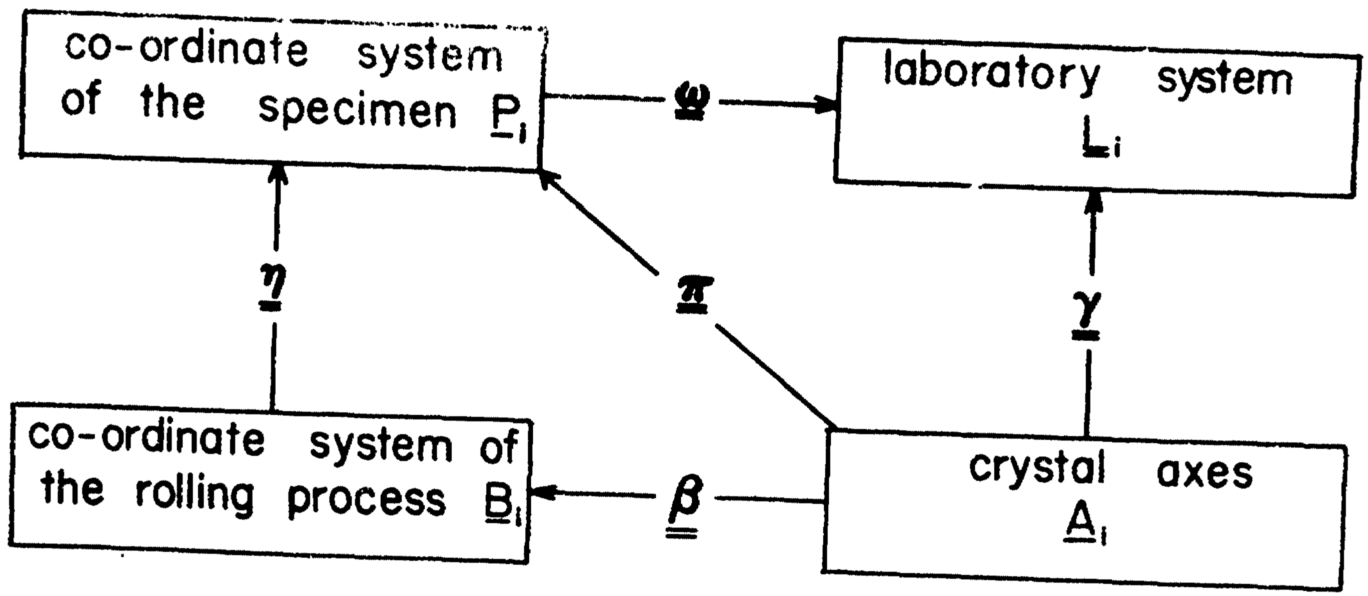

Fig. 2 H. Dölle and J. B. Cohen

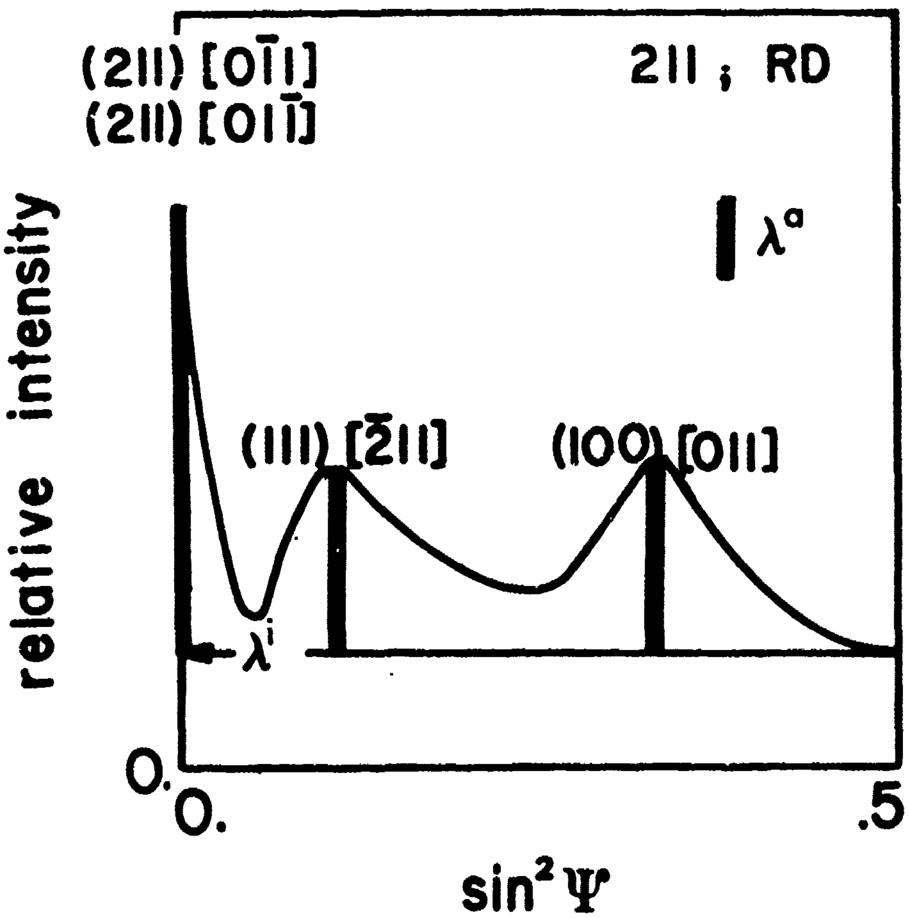

Fig. 3 H. Dölle and J. B. Cohen

fig 3.

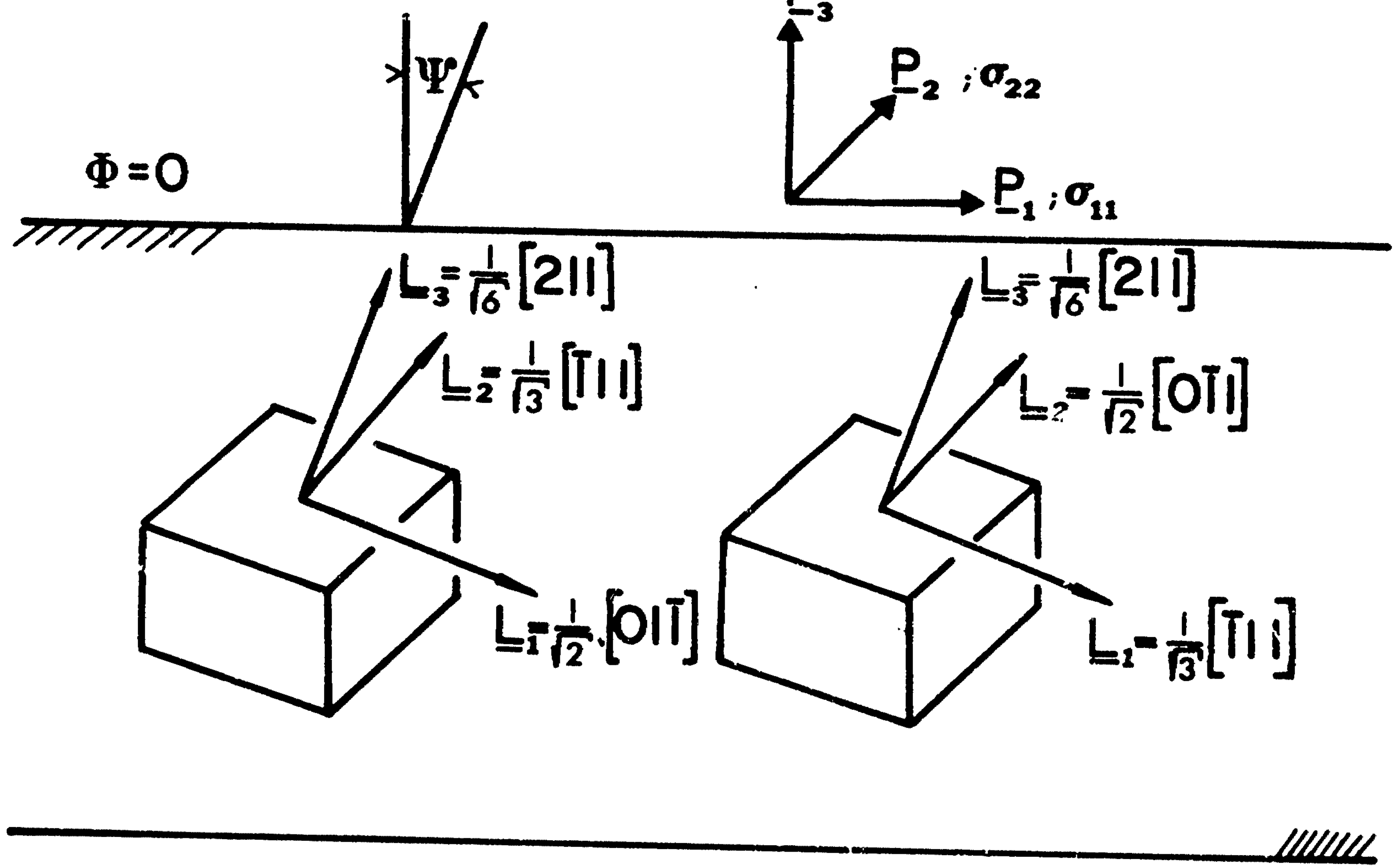

fig. 4

Fig. 4 H. Dölle and J. B. Cohen

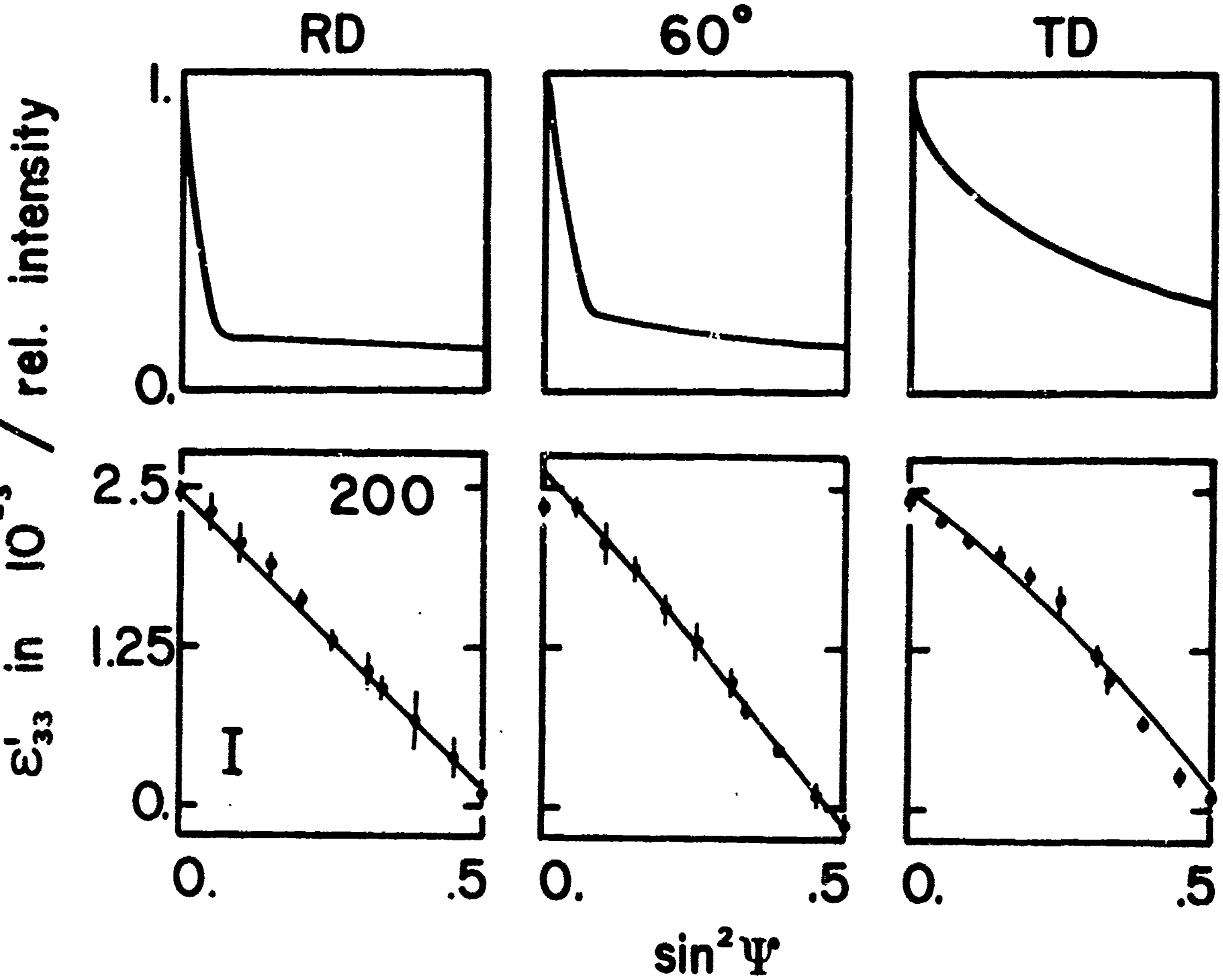

Fig. 5 H. Dölle and J. B. Cohen

fig. 5

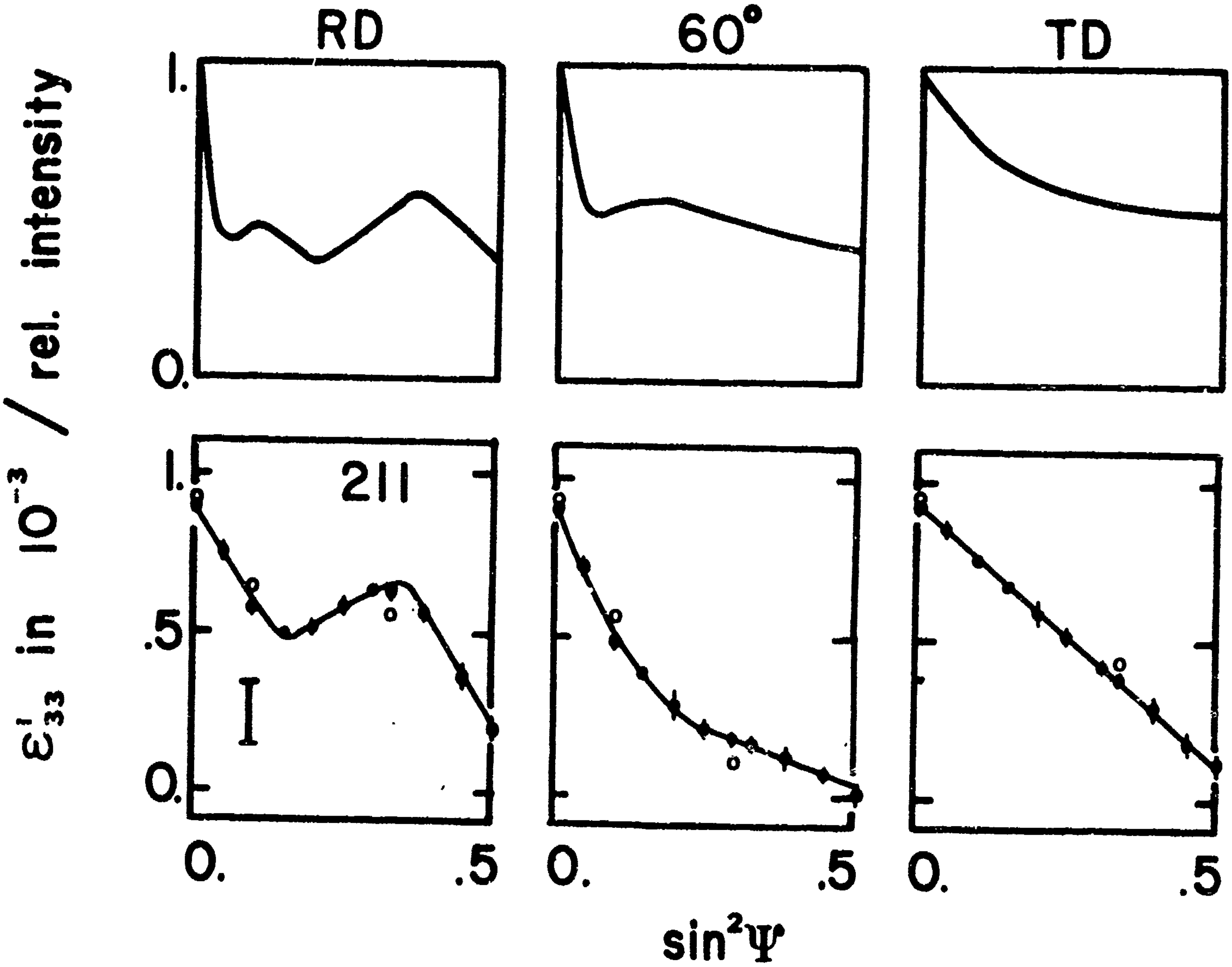

Fig. 6 H. Dölle and J. B. Cohen

fig. 6

Unclassified

Security Classification

DOCUMENT CONTROL DATA - R & D

(Security classification of title, body of abstract and indexing annotation must be entered when the overall report is classified)

1. ORIGINATING ACTIVITY (Corporate author)

J. B. Cohen
Northwestern University
Evanston, Illinois 60201

2a. REPORT SECURITY CLASSIFICATION

Unclassified

2b. GROUP

3. REPORT TITLE

6

ANOMALIES IN X-RAY RESIDUAL STRESS MEASUREMENTS IN COLD-ROLLED STEELS

4. DESCRIPTIVE NOTES (Type of report and inclusive dates)

9 Technical Report, No. 25 14 TR-25

5. AUTHOR(S) (First name, middle initial, last name)

10 Heiner Dölle and Jerome B. Cohen 12 29p.

11

6. REPORT DATE

7 September 7, 1979

7a. TOTAL NO. OF PAGES

26

7b. NO. OF REFS

26

8a. CONTRACT OR GRANT NO.

15 N00014-75-C-0580, NSF-DMR76-8984

9a. ORIGINATOR'S REPORT NUMBER(S)

25

b. PROJECT NO.

NR 031-733, Mod. No. P00005

c.

9b. OTHER REPORT NO(S) (Any other numbers that may be assigned this report)

d.

10. DISTRIBUTION STATEMENT

Distribution of this document is unlimited

11. SUPPLEMENTARY NOTES

12. SPONSORING MILITARY ACTIVITY

Metallurgy Branch
Office of Naval Research

13. ABSTRACT

psi

In residual stress measurements with x-rays, the interplanar spacing is assumed to alter monotonically with the tilt (ψ) of the specimen to the x-ray beam; the calculation of the stresses is based on this assumption when either the well-known two-tilt or $\sin^2\psi$ methods are employed. But in materials with strong texture, large oscillations have sometimes been reported. A method proposed in the literature for evaluating stresses in such a situation as resulting from anisotropy has been tested and shown to provide a reasonable stress system; the texture must be known in detail, so as to calculate the effective elastic constants. More importantly, the theory predicts that the simpler methods and measured x-ray elastic constants can be used, and without knowledge of the texture, if hoo and hhh reflections are employed; this has been verified experimentally in this study. It is recommended that such reflections be employed in the future, rather than the common ones now utilized.

sin sq

DD FORM 1473 (PAGE 1)
1 NOV 65

S/N 0101-807-6801

260810

Unclassified

Security Classification

1/B

Unclassified

Security Classification

14 KEY WORDS	LINK A		LINK B		LINK C	
	ROLE	WT	ROLE	WT	ROLE	WT
residual stresses, x-ray measurements of stresses, anisotropy and measurements of stress						

DD FORM 1 NOV 65 1473 (BACK)
(PAGE 2)

Unclassified

Security Classification